Journal of Alloys and Compounds 508 (2010) 28–36

Contents lists available at ScienceDirect

Journal of Alloys and Compounds

journal homepage: www.elsevier.com/locate/jallcom

Ferromagnetic spin fluctuations in quasi-2D—$EuCu_9Mg_2$

A. Mauger[a,*], D. Ravot[b], P. Bonville[c], P. Solokha[d], S. De Negri[d], V. Pavlyuk[e,f], A. Saccone[d], J.-C. Tedenac[b]

[a] Université Paris-6, UMR7590, Institut de Minéralogie et Physique de la Matière Condensée, 140 rue de Lourmel, 75015 Paris, France
[b] PMOF, ICG UMR 5253, Université Montpellier II, 34000 Montpellier, France
[c] CEA-CE Saclay, Service de Physique de l'Etat Condensé, 91191 Gif-sur-Yvette, France
[d] Dipartimento di Chimica e Chimica Industriale, Sezione di Chimica Inorganica e Metallurgia, Università di Genova, Via Dodecaneso 31, I-16146 Genova, Italy
[e] Department of Inorganic Chemistry, Ivan Franko National University of Lviv, Kyryl and Mefodiy str. 6, 79005 Lviv, Ukraine
[f] Institute of Chemistry and Environment Protection, Jan Dlugosz University, al. Armii Krajowej 13/15, 42200 Czestochowa, Poland

ARTICLE INFO

Article history:
Received 24 June 2010
Accepted 16 August 2010
Available online 26 August 2010

PACS:
75.30.Mb
75.40.−s

Keywords:
Magnetic properties
Rare-earth compounds
Cluster glass

ABSTRACT

The ternary intermetallic compound $EuCu_9Mg_2$ has been synthesized. The magnetic properties have been investigated by magnetization measurements and ^{151}Eu Mössbauer spectroscopy. Europium is divalent and a spin freezing is observed at 25 K. However, this spin freezing is characterized by the onset of strong magnetic irreversibility, which suggests a cluster-glass freezing. The Mössbauer spectra can be analyzed as the superposition of two subspectra of Eu^{2+} ions, which is consistent with a cluster-glass freezing. A transition to the ferromagnetic state is induced by application of a magnetic field the order of 0.5 T. This anomalous feature is attributed to quantum spin fluctuations that oppose the long-range ferromagnetic ordering, due to the two-dimensional topology of the geometric arrangement of the Eu^{2+} ions. This 2D-topology is also evidenced by a quadratic variation of the specific heat as a function of temperature down to 2.7 K. The electrical resistivity is also analyzed in the framework of intermetallic compounds dominated by ferromagnetic spin fluctuations above the spin-freezing temperature.

1. Introduction

Aiming to improve hydrogen storage materials, many investigations have been performed on new ternary phases based on binary RM_n (R = rare-earth or transition metals, M = transition metals) [1]. Among them, the RM_9 family has attracted interest since the report by Kadir et al. [2] on the existence of RNi_9Mg_2 (R = La to Gd) compounds, the crystal structure of which can be viewed as stacking of $CaCu_5$ and $MgCu_2$ structure-type blocks. Later Solokha et al. [3] have synthesized the RCu_9Mg_2 series with R = Y, La–Nd, Sm–Ho and Yb. These compounds crystallize in an ordered superstructure related to the $CeNi_3$ structure type (containing $CaCu_5$ and $MgZn_2$ structure-type fragments).

The crystal structures of the RNi_9Mg_2 and RCu_9Mg_2 series are not identical, although related, so that the physical properties are different. Only few studies have been devoted to the physical properties of RCu_9Mg_2, although atypical behaviors could be inferred. The temperature dependence of the specific heat and the magnetic susceptibility of $CeCu_9Mg_2$ have been studied by Ito et al. [4] and Nakamori et al. [5], respectively. These authors have shown that $CeCu_9Mg_2$ is a heavy-fermion compound with a long-range antiferromagnetic ordering, in a Fermi-liquid state below 2.7 K. This long-range order is confirmed by the anomalies detected in $\rho(T)$ and $C_p(T)$. In $CeCu_9Mg_2$, the hexagonal crystal field splits the ground state of Ce^{3+} in three Kramers doublets revealed by a Schottky anomaly around 30 K. The γ coefficient is relatively large – 160 mJ/K^2 – reflecting an enhancement of the electron mass [5]. Specific properties of $CeCu_9Mg_2$ could be explained by a two-dimensional arrangement of the cerium ions. However, this two-dimensional description is more or less in contradiction with the analysis of $C_p(T)$ based on a splitting of the ground state of the Ce^{3+} ion by the three-dimensional hexagonal symmetry. The large value of γ makes this compound promising for applications in thermoelectricity.

Among the RCu_9Mg_2 series, the Eu-compound has attracted our interest because, if europium is in the divalent state, and we show in this work that such is the case, its orbital momentum vanishes and crystal field effects are negligible. We could then have expected a simpler magnetic structure. However, our measurements reveal a rather complex behavior. It is the aim of this paper to shed light on it.

2. Experimental

Detailed information about sample synthesis has been published previously [3]. The samples were characterized using conventional methods. The microstructure and composition were investigated by applying the optical microscopy (by a DM4000M, Leica Microsystems, Wetzlar, Germany), scanning electron microscopy and energy-dispersive X-ray spectroscopy (EDXS) (*EVO 40*, Carl Zeiss SMT Ltd., Cam-

* Corresponding author.
E-mail address: alain.mauger@impmc.jussieu.fr (A. Mauger).

0925-8388/$ – see front matter © 2010 Elsevier B.V. All rights reserved.
doi:10.1016/j.jallcom.2010.08.059

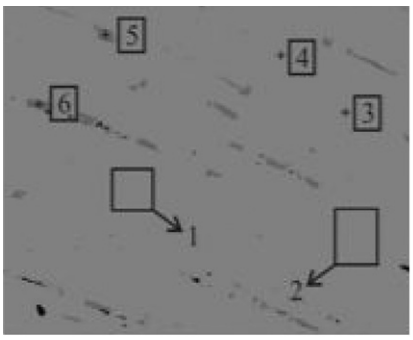

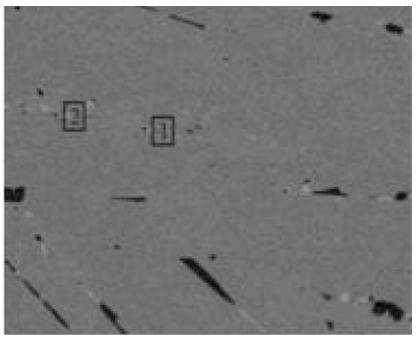

	Mg	Cu	Eu	Phase identity
1	16.8	75.2	8.0	$\|EuCu_5Mg_2$
2	17.2	74.5	8.3	$\|EuCu_5Mg_2$
3	16.7	74.9	8.4	$\|EuCu_5Mg_2$
4	16.1	75.7	8.2	$\|EuCu_5Mg_2$
Mean	16.7	75.1	8.2	
5	32.5	66.6	0.8	Cu_2Mg
6	31.8	67.1	1.1	Cu_2Mg

	Mg	Cu	Eu	Phase identity
1	0.43	83.19	16.38	$EuCu_5$
2	2.05	82.46	15.48	$EuCu_5$

Fig. 1. Electron microscope image of sample 1. The results of the analysis in selected area identified by numbers are reported below the corresponding image. The rectangle means that the measurements were not performed in the point-mode, but in scan-mode, and the results of composition presents the average composition within the margins of rectangle. In any case all our data even those "points" or "rectangles" correlate well.

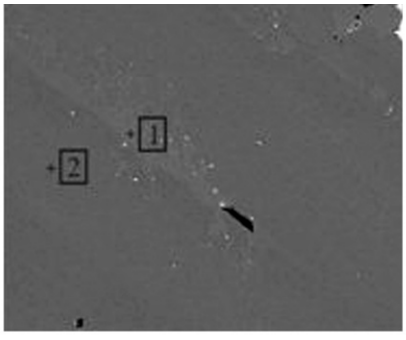

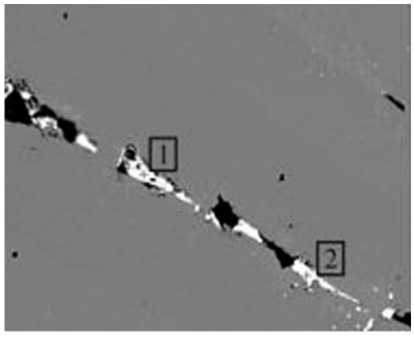

	Mg	Cu	Eu	Phase identity
1	16.68	74.72	8.60	$EuCu_5Mg_2$
2	16.99	74.78	8.23	$EuCu_5Mg_2$
Mean	16.84	74.75	8.41	

	Cu	Eu	Phase identity
1	68.46	31.54	EuCu2
2	69.51	30.49	EuCu2
Mean	68.99	31.01	

Fig. 2. Same as Fig. 1, for sample 2.

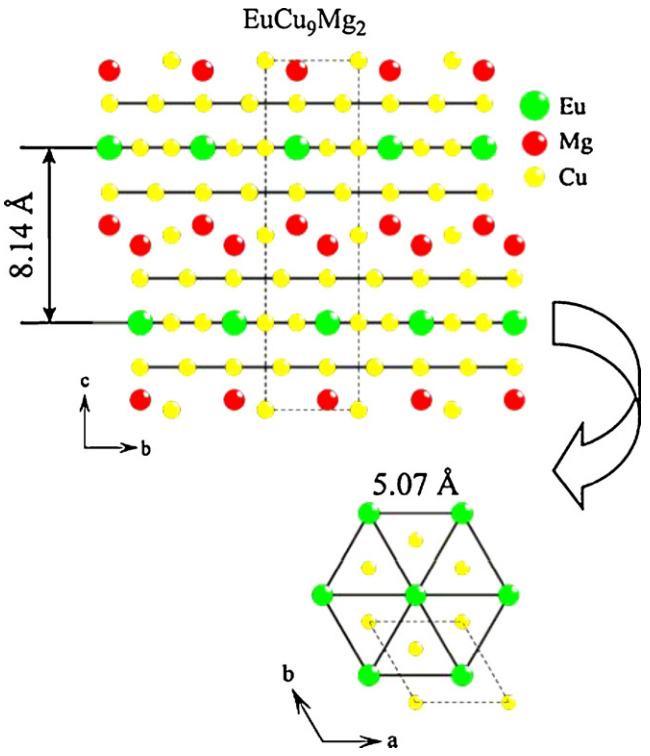

Fig. 3. Crystallographic structure of $EuCu_9Mg_2$ emphasizing the Eu^{2+} planes.

bridge, England). X-ray diffraction on powdered samples was performed by means of diffractometer Philips *X'Pert* MPD (Cu-Kα radiation, step mode of scanning) in order to ensure the crystal structure of $EuCu_9Mg_2$ phases. Rietveld matrix full profile structure refinements were carried out using the FULLPROF software [6].

Magnetic susceptibility and magnetization measurements were conducted on the polycrystalline samples of $EuCu_9Mg_2$ using a SQUID magnetometer from Quantum Design. Analyzed samples were crushed into pieces, fixed by glass wool into gelatin capsule, further sealed in polypropylene tube and placed into the magnetometer. The data were collected in the temperature range 3–300 K with magnetic flux densities up to 7 T.

Mössbauer spectroscopy experiments on the isotope ^{151}Eu were performed using a Sm^*F_3 γ-ray source mounted on a linear velocity electromagnetic drive in the temperature range 4.2–160 K, with a particular emphasis around 30 K. For ^{151}Eu, the "velocity unit" 0.1 cm/s corresponds to a frequency of 17.36 MHz.

The heat capacity was measured in a commercial semi-adiabatic system under high (10^{-6} mbar) vacuum in VSM (Oxford Instruments) above 9 K. Additional heat capacity measurements on $EuCu_9Mg_2$ were performed in ICMB by a relaxation method with a Quantum Design PPMS system and using a two τ-model analysis. Data were taken in the 2–50 K temperature range. For these latter measurements, the sample was a plate (37.7 mg weight).

3. Synthesis and characterization

Two samples (referred as sample 1 and sample 2) from two different batches were used in this study, to separate intrinsic from extrinsic properties. The results of the quantitative chemical analysis (EDXS) correspond to average compositions $EuCu_{9.11}Mg_{2.02}$ and $EuCu_{9.15}Mg_{2.05}$ for sample 1 and sample 2, respectively, close to the ideal 1:9:2 stoichiometry. In addition, the variation in composition determined in different spots is very small, so that the samples can be considered as homogeneous, except for very small amounts of secondary phases: sample 1 contains $EuCu_5$ and Cu_2Mg (Fig. 1), and sample 2 contains only $EuCu_2$ (Fig. 2). In both cases, these secondary phases were not detectable by X-ray diffraction experiments. The results of the Rietveld refinements have been published in our prior work [3].

Fig. 3 shows the crystallographic structure of $EuCu_9Mg_2$ emphasizing the 2D dimensional arrangement of the europium ions. $EuCu_9Mg_2$ contains two Eu-layers per unit cell distanced by 8.14 Å.

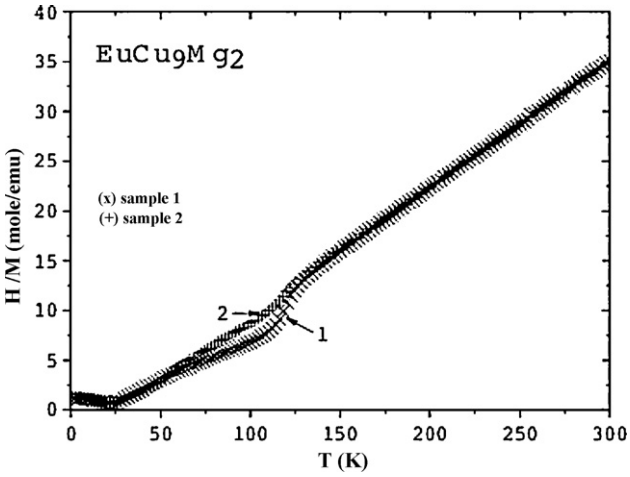

Fig. 4. Thermal dependence of the inverse of the magnetic susceptibility χ of the two $EuCu_9Mg_2$ samples. In this figure, χ is defined as M/H with M the magnetization measured in zero-field-cooled conditions, the magnetic field applied after cooling is $H = 0.1$ T.

Every europium ion inside these layers has six nearest neighbors in the form of an ideal hexagon, at equidistance 5.07 Å.

4. Magnetic properties

4.1. Static properties

The temperature dependence of the inverse magnetic susceptibility $1/\chi$ of the samples 1 and 2 is reported in Fig. 4. In this figure, χ is defined as the ratio M/H where M is the magnetization measured in an applied field $H = 0.1$ T. Above 150 K, $1/\chi$ follows a Curie–Weiss law from which we can deduce an effective magnetic moment $\mu_{eff.} = 7.92\,\mu_B$ equal to the value expected for the free Eu^{2+} ion so that europium is divalent in this compound. The paramagnetic temperature is $\Theta_p = 24.4$ K, which reveals the presence of ferromagnetic interactions between Eu^{2+} ions. At 120 K an anomalous decrease of $1/\chi$ is observed. To explore the origin of the anomaly at 120 K, the magnetization curves have also been investigated. A selected set of them is shown in Fig. 5. As expected, the magnetization M is linear in H up to the highest field investigated at $T > 120$ K, which validates our definition of the magnetic susceptibility as M/H. However, in the temperature range $80 < T < 120$ K, the magnetization is linear in H only in the high field range, typically $H \geq 2$ T. This is the signature of a ferromagnetic impurity. In this scheme, the magnetization at temperatures $80 < T < 120$ K can be decomposed in two components [7]. The extrinsic part is due to the ferromagnetic nano-clusters in concentration N, which carry a large magnetic moment M_s that is easily aligned along a magnetic field smaller than 1 T. The intrinsic contribution to the magnetization is linear in H, and is responsible for the linear variation when the extrinsic one has saturated to $NM_s(T)$ at $H \geq 2$ T. The intrinsic magnetic susceptibility is then $\chi_i = dM/dH$ ($H \geq 2$ T). The impurity phase responsible for the extrinsic part orders ferromagnetically (or ferrimagnetically) at 120 K. This precludes the possibility that the secondary phase is EuO, often met in europium compounds due to the oxidization of the powder during handling, like in $Eu_3Cu_8Sn_4$ [8], since the Curie temperature of EuO is 69 K. We are not aware of any europium compound that orders magnetically at 120 K, so that we do not preclude the possibility that the nano-clusters originate from defects rather than a secondary phase. Indeed, the material is lamellar, and this geometry is favorable to the formation of ferromagnetic clouds around a localized defect. $LiNi_{0.5}Mn_{0.5}O_2$ is an example [9]. In any case, the anomaly at 120 K

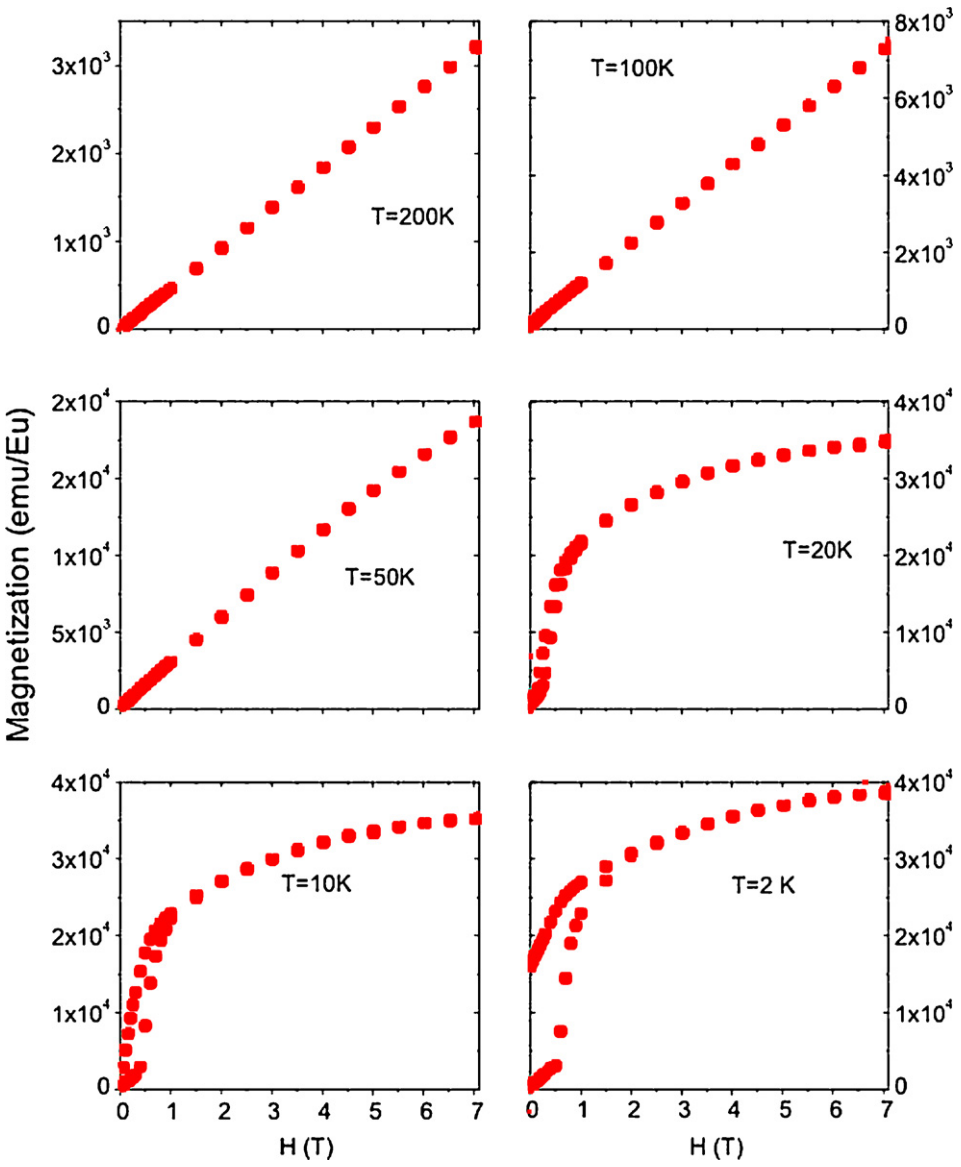

Fig. 5. Magnetization curves of $EuCu_9Mg_2$ at different temperatures. The straight lines at $T = 100$ and 50 K are guides for the eyes, and are linear fits of the magnetization curves at high field. Below 50 K, magnetic irreversibility is observed, evidenced by the difference between zero-field-cooled and field-cooled data, shown in the figure.

is clearly of an extrinsic origin. This is confirmed by the fact that the thermal evolution of the lattice parameter (not shown) does not reveal any crystallographic transition in this temperature range. In addition, the anomaly is more or less important depending on the samples, which is another evidence for an extrinsic effect. This is illustrated in Fig. 4, which shows that the anomaly is reduced in the sample 2. Note the relation $M/H \approx \chi_i(T) + NM_s(T)/H$ at large magnetic field below 120 K implies that M/H overestimates the intrinsic magnetic susceptibility $\chi_i(T)$. This is the reason for the drop of the $H/M(T)$ curve at 120 K. On the other hand, the magnetic properties below 50 K are the same in the different samples and are thus intrinsic. The reason is that $\chi_i(T)$ increases upon cooling, so that the extrinsic contribution that is saturated at NM_s ($T = 0$) becomes negligible at $T \leq 50$ K. For the same reason, the deviation of $H/M(T)$ with respect to the Curie–Weiss law extrapolated from high temperature decreases upon cooling in the intermediate regime $50 < T < 100$ K; the large deviation of $H/M(T)$ in this temperature range is attributable to the extrinsic component: the intrinsic magnetic susceptibility $\chi_i(T)$ satisfies approximately the Curie–Weiss law in the whole range $T > 40$ K. This is actually expected since important deviations with respect to the Curie–Weiss law due to local spin correlations are expected at $T < 2\Theta_p$ only.

On the other hand, the magnetic ordering at $T_c = 25$ K evidenced by the opening of the hysteresis cycle in Fig. 5 is an intrinsic property of $EuCu_9Mg_2$. Note, however, that the magnetization at $T < T_c$ is proportional to H as long as the applied field remains lower than some critical value H_c. This behavior shows that in this low-field range, the sample is not yet in a homogeneous ferromagnetic state. The transition to the ferromagnetic state is induced by the application of the finite field H_c, which is characterized by the sharp increase of the magnetization. At $T = 2$ K where $H_c \approx 0.5$ T, the saturation of the magnetization is almost complete at $H = 7$ T, leading to a magnetic moment of 7.16 μ_B/Eu in reasonable agreement with the expected value (7 μ_B) for Eu^{2+} free ions. Therefore, both the effective magnetic moment in the paramagnetic regime and the moment at saturation in the ferromagnetic state confirm the composition of the sample. They also show that Eu is divalent at all temperatures in this compound.

At $H < H_c$, the zero-field-cooled (ZFC) magnetic susceptibility curve goes through a maximum at T_c, which can be viewed as a

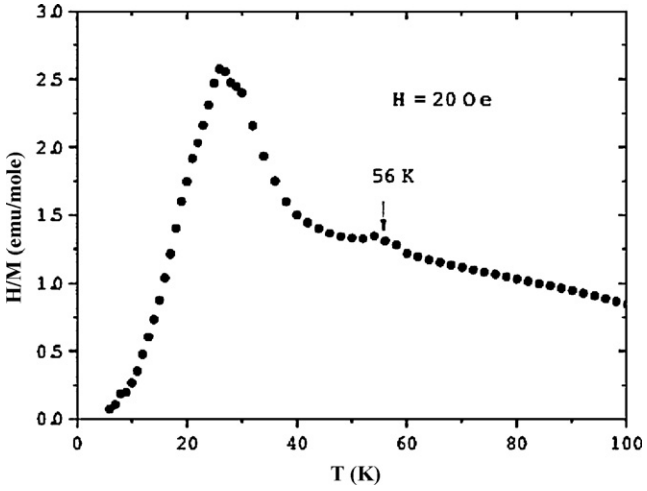

Fig. 6. Low temperature thermal dependence of the magnetic susceptibility (sample 1), defined in this figure as M/H with M the magnetization measured in zero-field-cooled conditions, the magnetic field is $H = 20$ Oe.

pre-transitional effect to the ferromagnetic phase that is observed at $H > H_c$, and the signature of a collective spin freezing. This is illustrated in Fig. 6 for $H = 20$ Oe. According to the ZFC procedure, the sample has been first cooled down to 2 K without any magnetic field, and the data have been recorded upon heating after application of the magnetic field $H = 20$ Oe. The field-cooled (FC) curve obtained upon cooling from room temperature under the same applied magnetic field is reported in Fig. 7 for both samples. The small anomaly at 56 K in Fig. 6 is due to the residual amount of $EuCu_5$ known to order magnetically at this temperature. This anomaly is barely visible in Fig. 7, due to the change in the scale imposed by the very large difference between FC and ZFC below T_c. The onset of magnetic irreversibility, however, takes place roughly at the ordering temperature of the $EuCu_5$ impurity. The small irreversibility in the range $T_c < T < 56$ K is attributable to the blocking of the magnetic moment of the ferromagnetic $EuCu_5$ nanoparticles. The large difference between FC and ZFC data taking place at circa 40 K, and the related maximum of the ZFC-magnetic susceptibility gives evidence of a collective spin freezing at T_c. However, instead of the static homogeneous magnetic moment polarized in a ferromagnetic arrangement observed at $H > H_c$, the spin freezing at $H < H_c$ is characterized by a broad distribution of relaxation times, like in the case of spin glasses or cluster glasses, as the magnetic properties

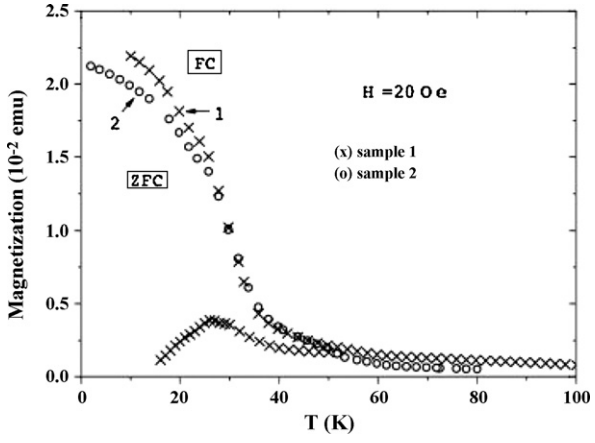

Fig. 7. Field-cooled magnetization ($H = 20$ Oe) at low temperature. The zero-field-cooled data for sample 1 are also reported for comparison.

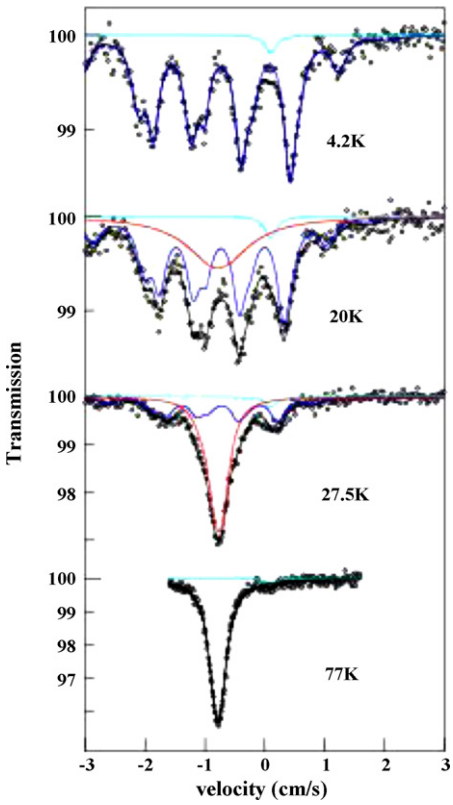

Fig. 8. Mössbauer absorption spectra on ^{151}Eu in $EuCu_9Mg_2$ at selected temperatures. The black curve is the fit, and the decomposition in two or three subspectra is as follows: the subspectrum in cyan corresponds to Eu^{3+}, the blue and red subspectra to Eu^{2+}. (For interpretation of the references to color in this figure legend, the reader is referred to the web version of the article.)

are qualitatively the same. The characterization of this spin freezing then requires the investigation of its dynamic properties.

4.2. Spin dynamics

4.2.1. Mössbauer spectroscopy

The europium neutron cross-section is very large (≈5000 b), which precludes any neutron diffraction experiments on natural europium compounds. To study the magnetic behavior of $EuCu_9Mg_2$, we have thus performed ^{151}Eu Mössbauer spectroscopy experiments as a function of temperature. The results are presented in Figs. 8 and 9.

Above 40 K, the spectra do not depend on temperature, and consist of a single line with isomer shift IS = −0.785(5) cm/s, characteristic of Eu^{2+}, plus a small intensity line (3%) with IS = 0.1 cm/s attributable to Eu^{3+} (see spectrum at 77 K in Fig. 8). The latter component is presumably due to oxidation at the surface of the material. No visible spectral change is observed around 120 K, which is another proof that the anomaly in the magnetic susceptibility curve at this temperature is not an intrinsic property. The Eu^{2+} component is better interpreted by introducing a small quadrupolar hyperfine interaction, with coupling parameter QS = 0.018 cm/s, typical for a paramagnetic phase.

Below 40 K, the spectra are more complex. At 4.2 K, a single magnetic hyperfine spectrum is observed, with a hyperfine field of 29.5 T, typical for Eu^{2+} in a magnetically ordered phase (Fig. 8). At 15 K and above, a fit with a single magnetic spectrum is no longer possible. An extra Eu^{2+}component is present, which, however, is not resolved: one can think of another hyperfine field spectrum or of a broad fluctuation induced line. The latter hypothesis yields the best fitting results (see red subspectrum at 20 and 27.5 K in

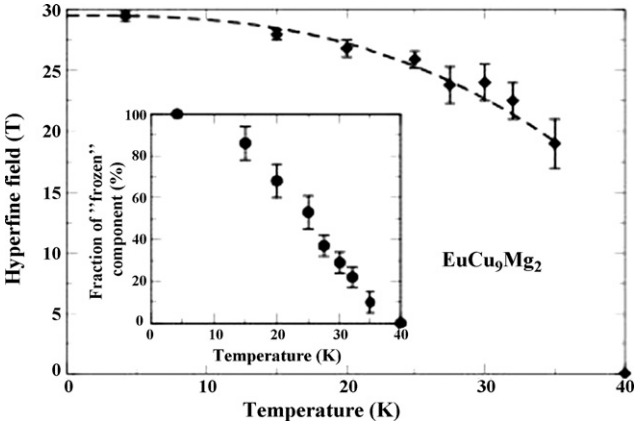

Fig. 9. Temperature dependence of the hyperfine field for the "frozen" Mössbauer component (blue subspectrum in Fig. 8) in $EuCu_9Mg_2$. Inset: thermal variation of its relative fraction.

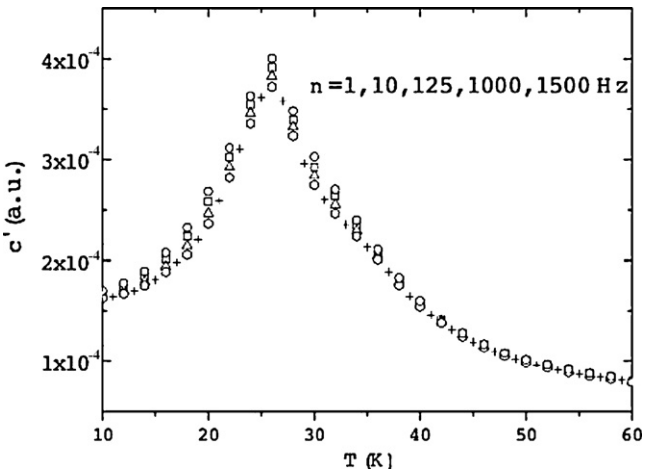

Fig. 10. Real part of the magnetic susceptibility χ' for different frequencies of the ac-field of amplitude 0.2 Oe. Data can be identified can be identified by the fact that, at given temperature, χ' decreases when frequency increases.

Fig. 8). The thermal evolution of this line is characterized by two phenomena, as temperature increases: (i) its intensity increases at the expense of that of the magnetic hyperfine spectrum (blue subspectrum in Fig. 8), and (ii) its width is constant up to 25 K, then it abruptly decreases at 27 K and above. We attribute the broad line to a component with a hyperfine field fluctuating at a frequency close to or higher than the ^{151}Eu hyperfine Larmor frequency $\nu_L \sim 200$ MHz. Since the hyperfine field is proportional to the Eu^{2+} magnetic moment, this line corresponds to fluctuating correlated Eu^{2+} spins. Thus, some Eu^{2+} spins start fluctuating fast (with respect to the Mössbauer time scale) deep in the ordered magnetic phase and the fraction of fluctuating spins increases with temperature, reaching about 50% at 25 K, which corresponds to the peak of the magnetic susceptibility. To understand this property, we note that in the (*ab*) plane of the hexagonal lattice, the europium sites form a triangular 2D-network (see Fig. 3). The site percolation threshold for the triangular lattice is 0.5. Therefore, the topology of this lattice implies that long-range magnetic order can take place only if the concentration of frozen spins exceeds this percolation threshold of 50%. Since this critical concentration is reached at $T_c = 25$ K (see Fig. 9), this temperature characterizes the onset of long-range magnetic ordering. The abrupt narrowing of the single line above 25 K corresponds to a drastic acceleration of the fluctuations that can also be taken as a signature of the magnetic transition, in quantitative agreement with the analysis of the magnetic properties in the previous section. Estimations of the spin fluctuation frequency yield around 400 MHz below 25 K and a few GHz above. As to the magnetically split subspectrum, it corresponds to "frozen" spins, in the sense that their fluctuations (if any) occur with a frequency lower than ν_L. The temperature dependence of their hyperfine field is shown in Fig. 9, together with the decrease of their relative weight as temperature increases. The determination of the hyperfine field is made difficult above 30 K due to the small intensity of this component, but the value of 18.5 T at 35 K is still high. It suggests the spin correlations are still strong at the short-range scale probed by the Mössbauer experiments, as expected in the temperature range $T_c < T < 2T_c$ where the Curie–Weiss law does not apply.

The coexistence of a magnetically split spectrum and a broad line deep in the magnetic phase is rather unusual, and it points to the presence of peculiar spin dynamics (or spin "freezing") at low temperature in $EuCu_9Mg_2$. Mössbauer spectroscopy gives access to the local magnetic properties and the spread of the coexistence region in the temperature range 15–35 K gives evidence that the magnetic spin freezing in the sample is very progressive and not homogeneous at the atomic scale. This result is fully consistent with the analysis of the magnetic properties at $H < H_c$ in the previous section, as expected since the Mössbauer experiments have been performed at $H = 0$. Since this spin-glass-like freezing is quite unusual for a sample that is well crystallized and not spin-diluted, we have explored further the spin-freezing dynamics by ac-magnetic measurements.

4.2.2. ac-Magnetic susceptibility

The real part $\chi'(T)$ and imaginary part $\chi''(T)$ of the ac-magnetic susceptibility have been measured in an ac-field of amplitude 0.2 Oe. The results are reported in Figs. 10 and 11, respectively, in the frequency range 1–1500 Hz. The peak of χ' at T_c does not significantly depend on frequency. This is the behavior characteristic of long-range magnetic ordering and at contrast with the canonical spin-glass freezing behavior. This result shows that the spin freezing is of a different nature, because of the proximity of the ferromagnetic freezing induced by an applied magnetic field $H > H_c$. The spin freezing is also evidenced by a broad maximum of $\chi''(T)$ in the temperature range 20–30 K. At 1500 Hz, a single maximum of $\chi''(T)$ is observed circa T_c as expected. At low frequency, however, the broad peak is split in two peaks centered at 30 and 20 K. This feature, together with the fact that no sharp behavior in the $\chi''(T)$ curve can be detected, suggests that the magnetic freezing is not homogeneous, which is consistent with the analysis of the Mössbauer spectra. Note the intensity of the broad peak in $\chi''(T)$ is not reduced as the frequency increases. The broad peak looks smaller at

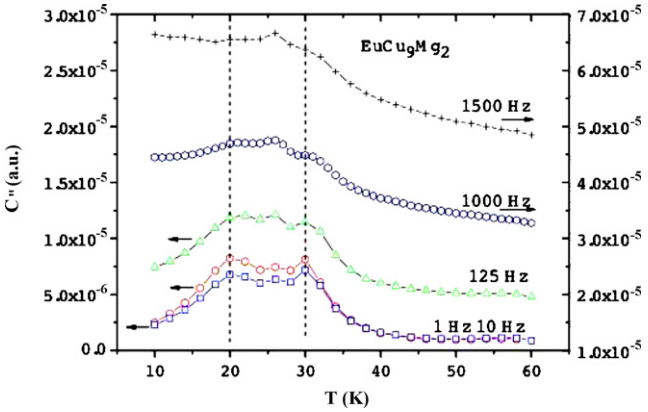

Fig. 11. Imaginary part of the magnetic susceptibility for the same frequencies as in Fig. 10.

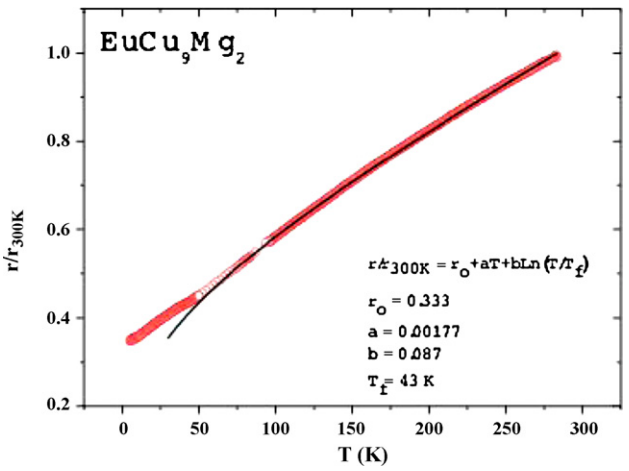

Fig. 12. Relative resistivity of $EuCu_9Mg_2$ as a function of temperature. The full line is a calculation according to Eq. (1).

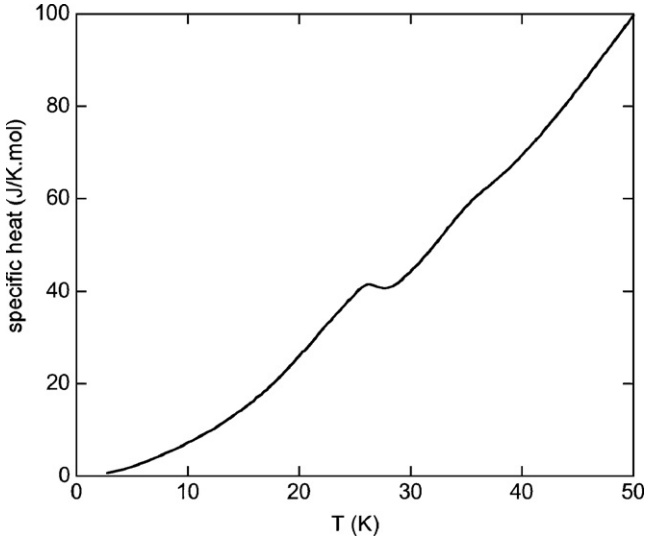

Fig. 13. Heat capacity C of $EuCu_9Mg_2$ as a function of temperature T.

1000 and 1500 Hz in the figure only because of the change of scale on the ordinate. This change of scale is due to the increasing background of the $\chi''(T)$ curve with the frequency of the ac-magnetic field, which reveals the progressive blocking of spins associated with the defects/impurities detected by the static measurements reported in the previous section.

5. Electronic and heat transport

5.1. A. Electronic resistivity

The thermal dependence of the relative resistivity is reported in Fig. 12. In the whole temperature range, ρ increases with T, showing that the sample is metallic. However, the $\rho(T)$ curve has a negative curvature in the whole paramagnetic regime. This is the typical behavior often met in systems dominated by spin fluctuations in a wide class of metallic compounds of d-transition elements and actinides [10]. In such a case, the saturation responsible for the negative curvature at high temperature is due to a logarithmic contribution predicted by the spin fluctuation theory [11]. We then follow our prior work on another intermetallic compound ($LaFe_4Sb_{12}$) dominated by ferromagnetic spin fluctuations, and write the resistivity under the form [12]:

$$\rho(T) = \rho_0 + aT + b\,\ln\left(\frac{T}{T_f}\right) \quad (T \geq T_f), \tag{1}$$

which holds true from high temperature down to a spin fluctuation temperature T_f (≈50 K) that compares well with $2T_c$. The S-shaped behavior is due to the existence of the inflexion point at T_f. In the present case, however, the onset of magnetic irreversibility at a temperature close to T_f prevents the observation of this inflection point. The contribution aT in Eq. (1) is a phenomenological term standing for the electron–phonon scattering used in the transport properties of metals with strong electron–phonon coupling [13]. The result of the fit is shown in Fig. 12 and is very good down to 50 K. Actually, the resistivity curve and the fit in Fig. 12 is very similar to the Fig. 4 in our prior work [12] on polycrystalline $LaFe_4Sb_{12}$. It also means that we meet the same problem encountered in this previous work, with a resistivity at low temperature that is large. This is due to the fact that we are dealing with poly-crystals, implying the existence of grain boundaries that may dominate the resistivity behavior. In $LaFe_4Sb_{12}$, the investigation of the resistivity curves on poly-crystals gives the results in [12] (same as in the present work), but the resistivity below the spin fluctuation temperature on single crystals is much lower [14] and the temperature dependence of the resistivity in this temperature range different from the results in poly-crystals. This result on $LaFe_4Sb_{12}$ illustrates that a quantitative analysis of ρ(T) below T_f can be done on single crystals only, and is thus beyond the scope of the present work.

5.2. Specific heat

The similitude in the transport properties between $EuCu_9Mg_2$ and $LaFe_4Sb_{12}$ dominated by ferromagnetic spin fluctuations is a motivation to explore the specific heat $C(T)$. In addition, the specific heat has over the electronic resistivity the great advantage that it is identical in poly-crystals and in single $LaFe_4Sb_{12}$crystals, and this is expected to be also the case in $EuCu_9Mg_2$. The reason is that the effect of impurities and defects on the specific heat at low temperature is negligible in ferromagnetic metals (except in the critical regime of a transition phase). It may be important in superconductors, due to the influence of impurities on the excitation gap [15], or in insulating alloys, and still only in very special cases leading to low-lying resonance modes [16], but not in rare-earth metallic compounds: see for instance [17].

The temperature dependence of the specific heat is reported in Fig. 13. $C(T)$ goes through a maximum at the spin ordering temperature T_c as expected, but in addition, a broad bump extends in the temperature region $30 \leq T \leq 40$ K. This is in agreement with the magnetic properties (see Fig. 7) and Mössbauer experiments (see Fig. 9) showing that a partial spin ordering already takes place at 40 K at low magnetic field. Note that the specific heat experiments, like the Mössbauer experiments, are made in the absence of applied magnetic field. To avoid the spurious effects of the critical spin fluctuations in the vicinity of T_c, we have analyzed the temperature dependence of $C(T)$ at temperature $T \leq 7$ K, down to the lowest temperature available in the experiments, 2.7 K. In this temperature range, the Log–Log plot in Fig. 14 shows that $C(T)$ satisfies a power law in T^n with $n = 2.0$, namely

$$C(T) \propto T^2. \tag{2}$$

This quadratic law gives evidence that the specific heat is dominated by the contribution of a Goldstone mode with linear dispersion in dimension $D = 2$. Such a contribution is expected to come from the "in-plane" vibrations of the lattice. In lamellar compounds, the crossover to the three-dimensional T^3 contribution of the lattice occurs at a temperature that increase when the C_{44} elastic coefficient decreases [18], and our result shows that this

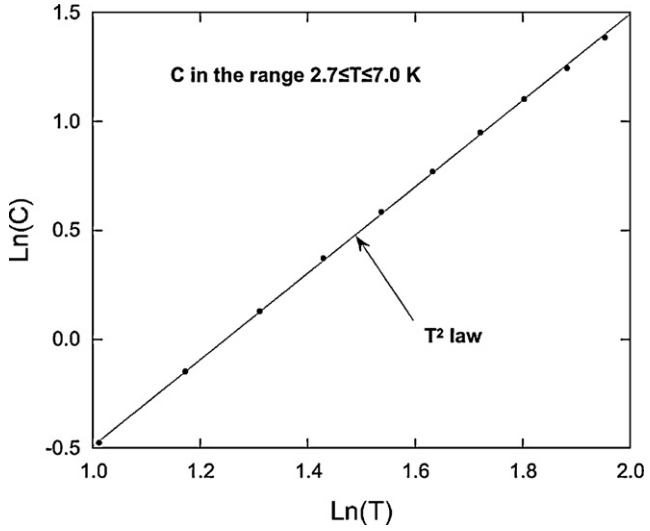

Fig. 14. Log–Log plot of the heat capacity. The full line is the quadratic law.

crossover occurs only at higher temperature, giving evidence of the two-dimensional character of the lattice already outlined in Fig. 1.

For a Heisenberg ferromagnet the contribution of the spin system to the specific heat is expected to be either in $T^{3/2}$ in $D = 3$, or in T in $D = 2$ [19]. A T^2 contribution can be observed in case of antiferromagnetic interactions in dimension $D = 2$, due to the existence of the Nambu–Goldstone mode, which has a gapless and linearly dispersive character [20]. Note, however, that the specific heat measurements have been performed without the application of any external magnetic field, so that the coherence length is limited to the size of magnetic domains, with frustration of the interaction in the inter-domain region. The magnetic contribution to the specific heat in that case might be close to that of 2D frustrated spin systems. In this case too a T^2 magnetic contribution to the specific heat has been observed, which is robust since it is not affected by impurities even in large concentrations, and even in the absence of any long-range magnetic ordering [21]. At this stage, it is then impossible to determine whether the specific heat is dominated by the phonons or the spin system, since both contributions might have the same temperature dependence. In any case, however, Eq. (2) is a property that is linked to the two-dimensional structure of the material already evidenced in Sections 1 and 3.

6. Discussion

Field-induced transitions have been observed in other quasi-2D systems such as $CeRhIn_5$ and Ce_2RhIn_8 [22]. However, they are antiferromagnets and they present spin-density waves in finite magnetic fields, at contrast with $EuCu_9Mg_2$ where the field-induced transition is ferromagnetic. On the other hand, field-induced ferromagnetic transitions can be observed in other materials, such as $(La_{0.4}Pr_{0.6})_{1.2}Sr_{1.8}Mn_2O_7$ [23], but the transition in this case is associated with a metal–insulator transition, i.e. the material is insulating and paramagnetic in the absence of a magnetic field, and the application of the magnetic field drives the transition to a metallic state, which restores a magnetic coupling mediated via the free carriers responsible for the onset of ferromagnetism. The situation here is quite different, since $EuCu_9Mg_2$ is metallic even in the absence of the magnetic field.

The physical properties are then quite unusual and they should be specific to quasi-2D systems with ferromagnetic interactions. Actually, a two-dimensional Heisenberg system does not order ferromagnetically, because of quantum fluctuations [24]. It is clear that $EuCu_9Mg_2$ cannot be considered as a truly 2D-Heisenberg ferromagnet. In particular, the magnetic susceptibility of a 2D-Heisenberg system with ferromagnetic exchange interaction J between nearest neighbors is [25]:

$$\chi = (3\pi JS)^{-1} \exp\left(\frac{4\pi JS^2}{kT}\right), \quad (3)$$

while we have shown that the Curie–Weiss law is observed in $EuCu_9Mg_2$. Magnetic coupling between the Eu-layers shown in Fig. 3 may restore a 3D spin ordering. The long-range inter-layer coupling has been shown to induce the three-dimensional ferromagnetic ordering at a Curie temperature comparable to that of T_c in different hybrid compounds [26]. The inter-layer coupling in that case was due to dipolar interactions. In the present material, such interactions should exist as well, but the RKKY indirect interactions mediated via the free carriers should play a role too. Usually, these interactions are sufficient to restore the Curie–Weiss law in the paramagnetic regime, but small enough to lead to anomalous spin-freezing properties. Such a situation has been met for instance in Ru/Rh metal graphite layered structure [27], or stage 2 $CoCl_2$ GIC [28,29].

6.1. Dynamics

The spin freezing with slow dynamics can be interpreted in terms of a cluster-glass freezing. Such a spin freezing is commonly observed in spin-diluted systems near the percolation threshold, even in the absence of the frustration of the magnetic interactions that drive the transition to the spin-glass phase for more spin-diluted systems. Among 3D-systems, an example is provided in $Fe_xMg_{1-x}F_2$ [30]. In such cases, magnetic clusters are formed at high temperature where they behave as superparamagnetic particles, and their fluctuations freeze out at the cluster-glass temperature. The image found in the literature in the case of quasi-two-dimensional systems is not much different despite the fact that the spins are not diluted; the magnetic clusters being referred to as islands [27–29]. In our case of a ferromagnetic quasi-2D system, we can envision the existence of magnetic domains with a size limited to the correlation length (that remains finite down to $T = 0$ for a 2D-Heisenberg ferromagnetic with interactions limited to nearest neighbors), or eventually the coherence length determined from the X-ray diffraction spectra if it is smaller than the coherence length. The common feature with the picture displayed in prior works is that the cluster-glass behavior is related to the finite size of the magnetic domains. The picture of magnetic "particles" or "islands" in quasi-2D systems, however, is deceptive, because a ferromagnetic particle would act as a macrospin, well located in space and with fixed magnitude (only the macrospin polarization can fluctuate under the application of a magnetic field), and we have shown in this work that the magnetic properties of $EuCu_9Mg_2$ are different. The reason is that we are not in a spin-diluted system, so that the finite size of the domain is not determined by the topology of the clusters of spins generated by spin-dilution. Instead, the magnetic domains fluctuate in time due to the spin dynamics inherent to the quasi-2D geometry. The spin dynamics of a cluster glass are then different from other systems. In particular, the Mössbauer spectrum in the cluster-glass state has the particular property that it can be decomposed in two subspectra that have been evidenced in $Fe_xMg_{1-x}F_2$ [31] above mentioned, just like the spin dynamics of $EuCu_9Mg_2$ probed by Mössbauer spectroscopy in the present work.

The spin dynamics investigated in the present work shows that the cusp in the ZFC-magnetic susceptibility does not shift significantly with the frequency of the ac-magnetic field. This is another difference with the spin dynamics of spin glasses, since the relative shift per frequency decade $\Delta T_c/[T_c \Delta \ln(\omega)]$ is in the range of 0.005 (Cu:Mn, Au:Mn) up to 0.08 ($FeMgCl_2$) [32], and

is even larger than 0.1 in the case of the freezing of superparamagnetic according to the Néel–Brown theory [33]. The lack of frequency dependence of the susceptibility cusp is then another proof that the spin freezing is a phase transition that is not associated with magnetic frustration effects. Indeed, the cusp of the ac-susceptibility in the quasi-2D ferromagnetic Ru-metal graphite system does not depend significantly on the frequency of the ac-field either [24].

6.2. Static properties and transport

The cusp of the zero-field-cooled magnetic susceptibility of $EuCu_9Mg_2$ is commonly observed in both the spin glasses and the cluster glasses. Actually, this cusp is invariably predicted for cooperative spin freezing [34,35]. On the other hand, the peak in the specific heat is more questionable. In spin glasses, there are claims that there is no anomaly at the spin-freezing temperature [36–38], and no anomaly is expected in case the freezing supports the picture of a viscous freezing rather than a spin-glass phase transition with cooperative freezing. On the other hand, for cluster glasses, all the theoretical models in which superparamagnetic clusters of spins order cooperatively, a peak in the specific heat $C(T)$ curve is expected, at the same temperature where the magnetic susceptibility cusp is observed [39–41]. This is also the case met in $EuCu_9Mg_2$, and the signature that the spin freezing is a collective phenomena, even if the spin fluctuations due to the quasi-2D geometry makes the spin-freezing inhomogeneous, as evidenced by the magnetic experiments and the Mössbauer spectroscopy.

The linear variation of the magnetization with the dc-field H at low temperature, followed by the sharp increase of the magnetization in the field-induced transition to the ferromagnetic state is reminiscent of the inflection point observed in the magnetization curves $M(H)$ of $Co_{1-x}Fe_xPt_3$ at Fe concentrations $x > 0.2$ in the region of the phase diagram where magnetic interactions are mainly ferromagnetic ($CoPt_3$ is a ferromagnet), but Fe introduces frustration ($FePt_3$ is an antiferromagnet) [42]. In this case, the inflexion point is interpreted as the transition to re-entrant spin-glass phase, which is also an inhomogeneous phase where ferromagnetic domains coexist with spin-glass domains [42], a picture actually close to that of the cluster glass. However, the magnetization has a positive curvature in this re-entrant spin-glass phase at low field, while the magnetization is roughly linear in H in $EuCu_9Mg_2$ at low field. Therefore the transition to the ferromagnetic phase in the present case is much sharper and suggests a field-induced phase transition, which can be attributed to the freezing of the spin fluctuations specific to the quasi-2D geometry by the application of the external magnetic field.

In conclusion, the magnetic, electronic, electric and heat transport properties of $EuCu_9Mg_2$ have been investigated and have revealed unusual behaviors that have been analyzed self-consistently. The analysis suggests that they are the fingerprints of the quasi-2D ferromagnetic systems.

Acknowledgments

We thank Florence Rullier-Albenque (CEA/SPEC) for performing the resistivity measurements, and Raphaël Hermann (Liège, Jülich) for fruitful discussions about the relaxational 151Eu Mössbauer lineshapes. We are also indebted to R. Decourt and B. Chevalier (CNRS, Université de Bordeaux, ICMCB) for the specific heat measurements.

References

[1] M. Latroche, A. Percheron-Guegan, J. Alloys Compd. 356–357 (2003) 461–468.
[2] K. Kadir, I. Uehara, T. Sakai, J. Alloys Compd. 257 (1997) 115.
[3] P. Solokha, V. Pavlyuk, A. Saccone, S. De Negri, W. Prochwicz, B. Marciniak, E. Różycka-Sokołowska, J. Solid State Chem. 179 (2006) 3073–3081.
[4] M. Ito, K. Asada, Y. Nakamori, H. Fujii, T. Fujita, T. Suzuki, Physica B 329–333 (2003) 482–483.
[5] Y. Nakamori, M. Ito, H. Fukuda, T. Suzuki, H. Fujii, T. Fujita, Y. Kitano, Physica B 312–313 (2002) 235–236.
[6] J. Rodriguez-Carvajal, FULLPROF SUITE, LLB Sacley and LCSIM Rennes, France, 2003.
[7] A. Ait-Salah, A. Mauger, C.M. Julien, F. Gendron, Mater. Sci. Eng. B 129 (2006) 232.
[8] D. Mazzone, P.L. Paulose, S.K. Dhar, M.L. Fornasini, P. Manfrinetti, J. Alloys Compd. 453 (2000) 24–31.
[9] N Amdouni, K. Zaghib, F. Gendron, A. Mauger, C. Julien, Ionics 12 (2006) 117.
[10] J.M. Lawrence, P.S. Riseborough, R.D. Parks, Rep. Prog. Phys. 44 (1981) 1.
[11] N. Rivier, V. Zlatic, J. Phys. F: Met. Phys. 2 (1972) L99.
[12] R. Viennois, S. Charar, D. Ravot, P. Haen, A. Mauger, A. Bentien, S. Paschen, F. Steglich, Eur. Phys. J. B 46 (2005) 257.
[13] D.W. Woodart, G.D. Gody, Phys. Rev. A 136 (1966) 166.
[14] W. Schnelle, A. Leithe-Jasper, H. Rosner, R. Cardoso-Gil, R. Gumeniuk, D. Trots, J.A. Mydosh1, Yu. Grin, Phys. Rev. B 77 (2008) 094421.
[15] S. Nishizaki, Y. Maeno, Z. Mao, J. Low Temp. Phys. 117 (1999) 1573.
[16] C.M. Hogan, Phys. Rev. 188 (1969) 870.
[17] H. Wada, T. Inoue, M. Hada, M. Shiga, Y. Nakamura, Phys. Status Solidi B 162 (2006) 407.
[18] W. De Sorbo, G.E. Nichols, J. Phys. Chem. Solids 6 (1958) 352.
[19] G.Z. Wei, A. Du, J. Magn. Magn. Mater. 127 (1993) 64.
[20] A.P. Ramirez, G.P. Espinoza, A.S. Cooper, Phys. Rev. B 45 (1992) 32505.
[21] Y. Nambu, S. Nakatsuji, Y. Maeno, J. Phys. Soc. Jpn. 75 (2006) 043711.
[22] A.L. Cornelius, P.G. Pagliuso, M.F. Hundley, J.L. Sarrao, Phys. Rev. B 64 (2001) 144411.
[23] F. Moussa, M. Hennion, F. Wang, A. Gukasov, R. Suryanarayanan, M. Apotsu, A. Revcolevschi, Phys. Rev. Lett. 93 (2004) 107202.
[24] N.D. Mermin, H. Wagner, Phys. Rev. Lett. 17 (1966) 1133.
[25] M. Takahashi, Phys. Rev. Lett. 58 (1987) 168.
[26] M. Drillon, P. Panissod, J. Magn. Magn. Mater. 188 (1998) 93.
[27] M. Suzuki, I.S. Suzuki, J. Walter, Phys. Rev. B 67 (2003) 094406.
[28] M. Suzuki, I.S. Suzuki, Phys. Rev. B 58 (1998) 840.
[29] M. Suzuki, I.S. Suzuki, J. Phys. C: Condens. Matter 14 (2002) 5583.
[30] J. Jaccarino, J.R. King, Physica A 163 (1990) 291, and references therein.
[31] J. Satooka, S. Morimoto, A. Ito, RIKEN Rev. 27 (2000) 31.
[32] J.A. Mydosh, Spin Glasses: An Experimental Introduction, Taylor & Francis, London, UK, 1993.
[33] W.E. Brown, Phys. Rev. 130 (1963) 1667.
[34] S.F. Edwards, P.W. Anderson, J. Phys. F: Met. Phys. 5 (1975) 965.
[35] D.J. Thouless, P.W. Anderson, R.G. Palmer, Philos. Mag. 35 (1977) 593, and references therein.
[36] L.F. Wenger, P.H. Keesom, Phys. Rev. B 11 (1975) 349.
[37] D.L. Martin, Phys. Rev. B 21 (1980) 1902.
[38] K.A. Mirza, J.W. Loram, J. Phys. F: Met. Phys. 15 (1985) 439.
[39] A. Smith, J. Phys. F: Met. Phys. 4 (1974) L266.
[40] C.M. Soukoulis, Phys. Rev. 18 (1978) 3757.
[41] C.M. Soukoulis, K. Levin, Phys. Rev. 18 (1978) 1439.
[42] T.H. Kim, M.C. Cadeville, A. Dinia, V. Pierron-Bohnes, H. Rakoto, Phys. Rev. B 54 (1996) 3408.